Journal of Ceramic Processing Research. Vol. 21, No. 5, pp. 539~546 (2020)
(Received 6 March 2020, Received in revised form 5 April 2020, Accepted 7 April 2020)
https://doi.org/10.36410/jcpr.2020.21.5.539

J O U R N A L O F
Ceramic Processing Research

Wear behavior of irregular shape Ti6Al4V powder reinforced with carbon nanotubes

Muhammet Ceylan[a,*] and İsmail Topcu[b]
[a]*Department of Mechatronics Engineering, Istanbul Commerce University, Istanbul, Turkey*
[b]*Department of Metallurgy and Materials Engineering, Alanya Alaaddin Keykubat University, Antalya, Turkey*

The purpose of this study was to investigate the sintering behavior, microstructural evolution, and the effect on wear resistance of carbon nanotubes (CNT) with the addition of a mechanical alloy (Ti6Al4V) and sintered irregular Ti64 powder. The mechanical alloy powders utilized in this study were produced through the process of CIP (Cold Isostatic Press) in order to produce samples by compress on under various pressures within a 300 MPa floating molded press. The samples were sintered at a high vacuum (10-5 mbar) for 60 minutes at a temperature of 1275 ºC. After sintering, the materials were characterized using an optic microscope (OM), scanning electron microscopy (SEM) and EDX (Energy-dispersive X-ray spectroscopy) to determine whether the materials had wear resistance, density measurement, etc. The Carbon Nanotube wear and friction behavior were investigated under various conditions using a pin wear tester on a disc followed by a scanning electron microscopy (SEM) analysis. The objective of this study was to evaluate the density, metallographic properties and hardness of Ti64 samples supplemented with different CNT ratios as a function of sintering temperature. Theoretical density and micro-hardness of mechanical alloyed and sintered irregular Ti64 powders changed with the additions to CNT under increased sintering temperatures.

Keywords: Sintering, Ti6Al4V, Carbon Nanotubes, Wear, Ti6Al4V Powder.

Introduction

Titanium alloys can be used in a wide variety of applications. A few examples include the biomedical, automotive and aerospace industries. Ti6Al4V alloy with 4% vanadium and 6% aluminum weight is preferred for use in surgical implants, turbines and airplanes because of its sufficient mechanical strength, heat treatment ability, good corrosion resistance, and biocompatibility. It is a powder metallurgy (PM) technique used in the production of titanium alloys and their composites [1-4]. As a result of the possibility of reinforcement in metal matrix composites, the properties of the composites can be changed and thus their applications can be extended. The *in situ* formation technique for changing the properties of composites provides the advantage of greater size and reinforcement control [5, 6].

Since the invention of the aircraft, the need of high strength and lightweight materials has been recognized and increased. When the hardness and strength of a material increases, the dimensions and therefore the mass of the material must also be reduced for a given load bearing application. This allows many advantages in automobiles and aircraft, such as increased load and improved fuel efficiency. The increase in fuel efficiency of engines has become an important issue due to the steady decline in global oil resources. The reason for the development of metal matrix composites (MMCs) is the inability of metals and alloys to provide a structure with both strength and hardness. The strength and ductility in the material are then provided by the metal matrix produced [7-9]. Titanium carbide (TiC) is used because of its compatibility and properties favorable in strengthening titanium alloy matrices [10]. Materials designed for particulate doped titanium matrix composites, bearings, abrasion resistant gears, erosion resistant pipes, shafts and friction resistant motors [11]. Component selection plays a significant role when it comes to the application of materials exhibiting the properties and characteristics needed for the production of titanium alloys and composites [12]. Titanium alloys are well known for their poor tribological properties [13-18]. In addition, titanium deforms very poorly on the opposite surface and easily transfers the material in the non-lubricated tribosystems. Furthermore, due to the great affinity of titanium to oxygen, it is easily transferred to both metallic and non-metallic surfaces that remain as polymers. This results in an oxide surface layer which in turn leads to severe adhesive wear. Under extreme fatigue terms at environmental temperature, force decrease factors between 2.6 and 3.6 were observed in titanium alloys as a result of the loss of the respective material [14]. Lastly, titanium alloys have weak wear resistance;

*Corresponding author:
Tel : +90 444 0 413-331
Fax: +90 (216) 489 02 69
E-mail: mceylan@ticaret.edu.tr

for example, Budinski [16] found that the dry sand rubber wheel for his wear test utilizing Ti-6Al-4V alloy and pure Ti to wear 15 times higher than D2 tool steel. This weak tribological conduct is attributed to the low hardness and absolute values of the tensile-shear strength of titanium and titanium alloys [17-24].

Carbon nanotubes (CNTs) were first discovered in 1991 by S. Iijema [25]. From a science and technology perspective, carbon nanotubes (CNTs) are on their way to becoming one of the fastest growing research areas in many disciplines including materials and life technologies, physics and chemistry. Unlike cast graphite and diamond, carbon nanotubes (CNTs) have unique optical, magnetic, electrical, mechanical, and thermal properties [26, 27]. Carbon nanotubes (CNTs) have interesting electrochemical properties as well. In the study by Hussain et al., it was found that the electroactivity of CNTs was due to the presence of surface reactive groups [28].

The purpose of this research is to investigate how the addition of 0.5% - 5% CNT has an effect on the wear properties of Ti64 P / M alloy. Metallographic techniques were used to characterize the CNT added as sintered samples. Each sample was subjected to abrasion tests with a pin on the disc. It was then characterized by, scanning electron microscopy (SEM), hardness tests, optical microscopy and X-ray diffraction (XRD). Worn surfaces of the sintered samples were analyzed under SEM.

Experimental Procedures

Raw materials and sintering process

In this study the Ti64 and CNT powders were purchased from industrial suppliers to do the first experiments and tested to determine their values. The purchase process; Ti64 and composite reinforced with 0.5% - 5% CNT 10-30 nm were used. The materials were fabricated (Phelly Materials Company) by a PM technique. As raw materials, atomized Ti64 powders having a purity density of 4.43 g / cm^3 and a nominal size of 45-180 99 μm were used. The materials used as matrix material were CNT and Commercially Ti64 powders. The reinforcement CNT material utilized in this study were (Chep Tubes Company and Choggo Company China - density 2.31 g/cm^3) particles. The CNT particle has a size of about 10-30 nm.

Production of composites

During the production of composites, 0.5% - 5% Volume CNT was reinforced to Ti64 by means of a tubular milling. Milling was performed for five hours. The ball / powder weight ratio was 6:1. The grinding speed was 400 rpm and the alumina ball diameter was 10 mm. Powder materials were easily pressed at 300 MPa by Cold Isostatic Press (CIP) process. The reason for its ease is because of the ceramic behavior of the CNT during the process. The selected sintering atmosphere was in high vacuum (1.2 10-5 mbar). Other sintering atmospheres may cause oxidation of TiO_2 material in the working rooms, so that the sintering of the samples was carried out at two different temperatures (1275 ºC).

Characterization

SEM is one of the most versatile tools available in the field of materials science, used to analyze the microstructural properties of materials. SEM sends a high energy electron beam to the sample surface and scans the surface and takes images. The powder morphology and microstructures of the prepared sintered samples were examined using a scanning electron microscope (SEM, JEOL Ltd., JSM-5910LV). Fig. 1. shows the morpholFig.ogies of the starting materials.

A Rigaku X Ray diffractometer was used to identify the phases in pure Ti64 powder and CNT powder from different companies as demonstrated in Fig. 2 with an incident angle of 2 ºC / Ka radiation. The angle of refraction was between 5-120º with a step increase of 0.02º and a counting time of 1 s. Energy Dispersive Spectrometer (EDS, OXFORD Industries INCAx-sight 7274, (133-eV resolution) were used to analyze material composition.

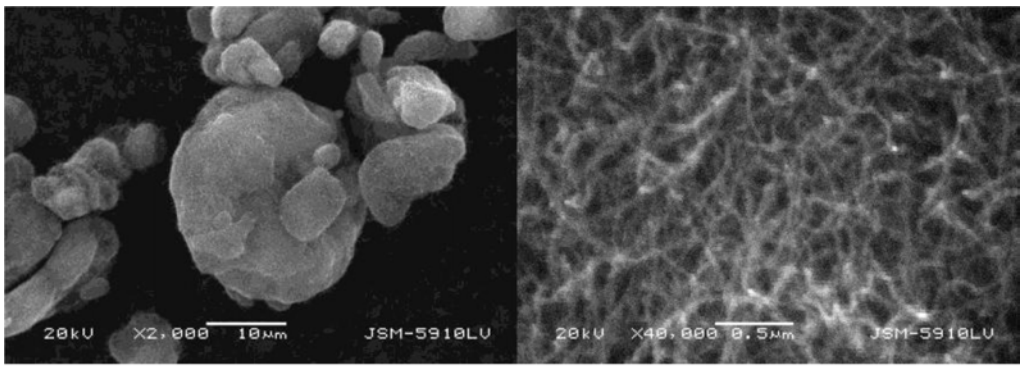

Fig. 1. SEM images of Ti64 and CNT powders: (a) Ti64 and (b) CNT.

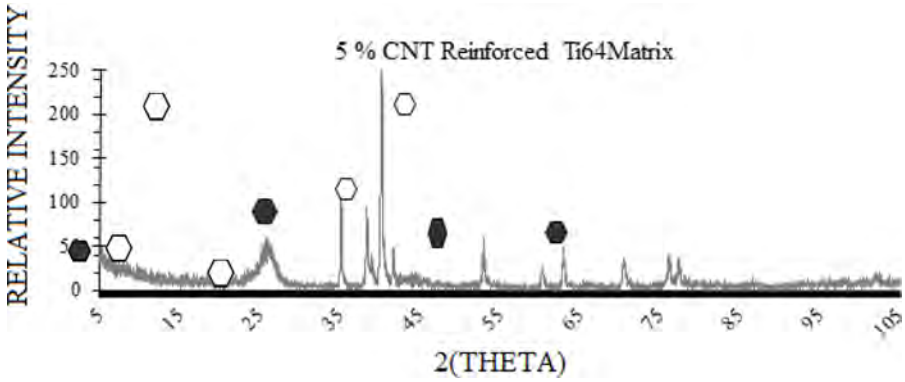

Fig. 2. XRD pattern of 5% content CNT particles in Ti64 Matrix.

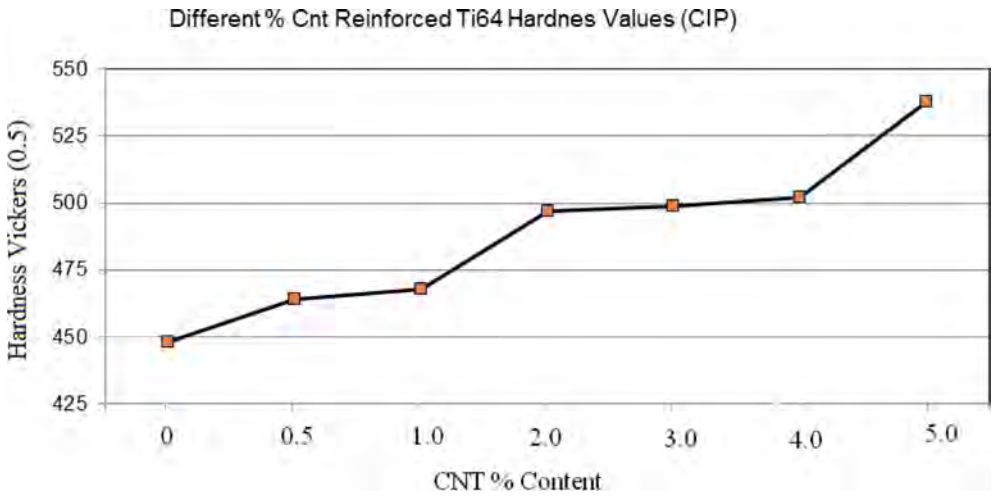

Fig. 3. The hardness versus different CNT content (0.5 - 5%).

Hardness and density experiments

The mechanical properties of the produced samples were determined with the help of hardness measurements. The hardness tests of the samples prepared by metallography were performed with a Micro-Hardness Tester Machine (FM-700, Future Tech Corp. in Japan). The Vickers 136º diamond in the metallographic samples was used to determine the hardness of the cutting compounds. Test load for each sample was 500 gr. Since the indentation trace covers both the matrix and the reinforcing material, the stiffness value shown represents the bulk stiffness of the composite. The results of these hardness tests were evaluated by taking the average of 10 consecutive test results. Hardness values with various CNT contents are demonstrated in Fig. 3.

The macro and micro-hardness measurements, which are referred to as hardness (HRC) (Wolpert Instron Corp. USA) were compared using the methods described within this section. There is an observed difference in the macro and micro surface hardness measurements; this significant difference in material phase change is thought to arise from the matrix material formed by the CNT material.

The Archimedes water immersion method was used to determine the densities of the sintered samples (Precisa XB 320M, Switzerland). Theoretical density measurements of the composite samples Ti64 /CNT in different proportions according to the literature ranged from 90 to 99.5%. The main reason for the variances of density measurements in the range from literature of these composites is the increased ratio CNT. Density calculations are presented in Fig. 4. The highest density of CNT, which had the lowest percentage of low density alloys, was found to have the highest CNT %. Selected composite samples are CNT-reinforced Ti64 powder produced by powder metallurgy. Information on the properties of the powders is provided in the previous section. The average density values of the composites containing different CNTs are shown in Fig. 4. Here, the densities of the specimens approximate the theoretical density with increasing sintering temperatures for the CNT contents in all ratios.

Metalographic examination

For metallographic examination, each sintered test

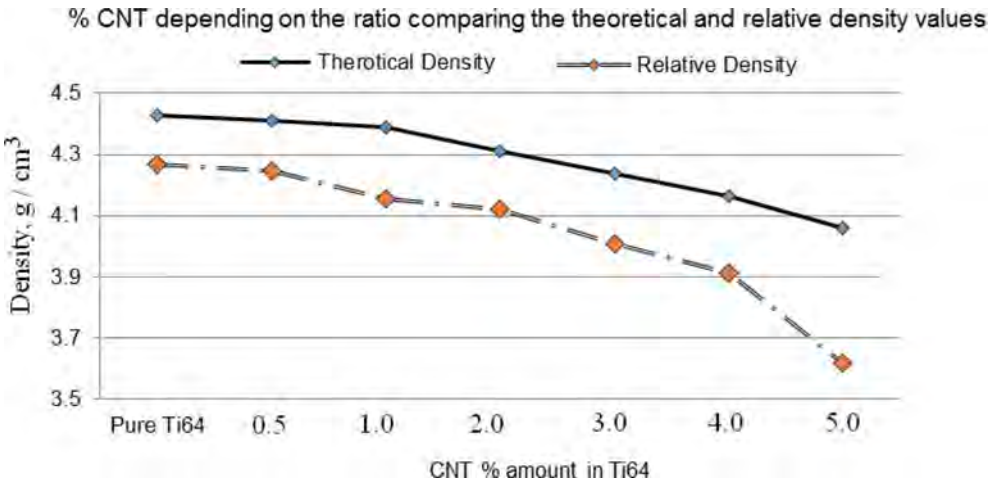

Fig. 4. CNT % reinforced by the density of different exchange rates.

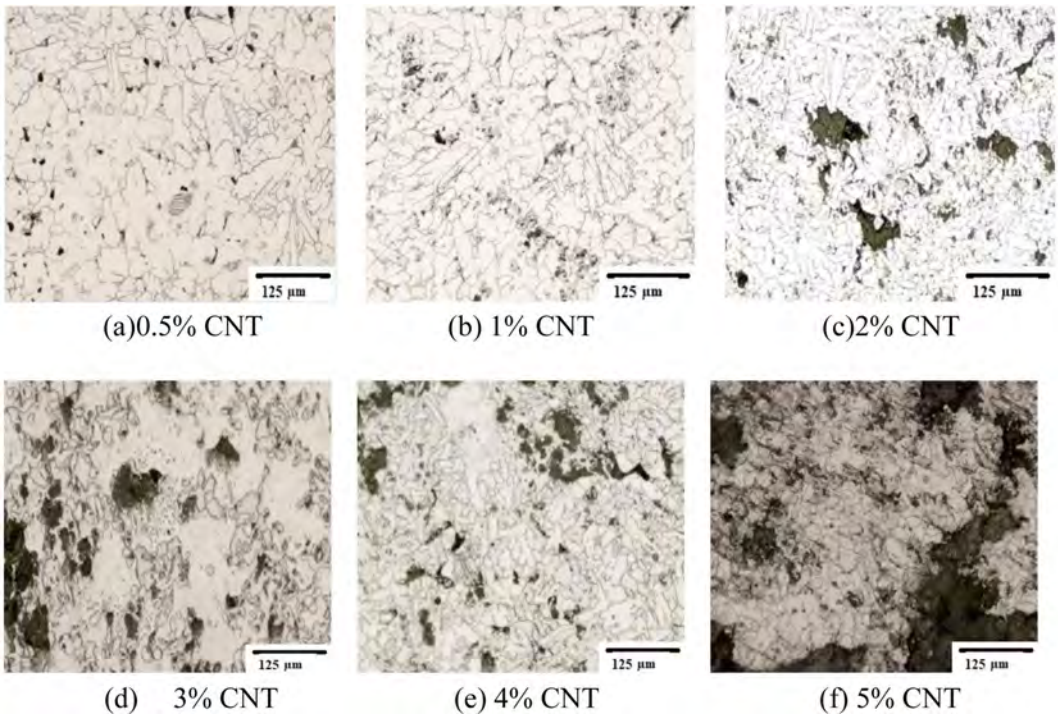

Fig. 5. Optical microscopy images of Ti64 (a), (b), (c), (d), (e) and (f) different reinforced CNT.

samples were evaluated for each composite material. A Kroll reagent (3 mL HF, 6 mL HNO_3 in 100 mL H_2O) was used to etch the samples for optical metallography. Prepared from longitudinal sections of composites after examination of metallographic samples. All samples were slowly ground with 240, 500, 800 and 1000 mesh SiC sand papers, respectively. In the next step, the samples were slowly polished with Kroll solutions. The microstructures of the composites were examined using Optimus Optic microscope. Metallographic images at different magnifications were taken for each sample after the sample preparation process (X50, X100 and X200), press and sections in the direction of the image.

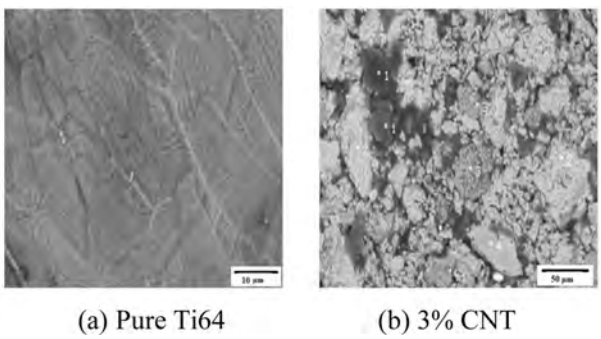

Fig. 6. SEM microscopy images of Ti64 (a) and (b) reinforced CNT.

Figs. 5 and 6 display these images. In these studies, the alpha and beta shows the structure of Ti64 powder. As seen in the figures, the images contain gray areas of TiC structures, the gray area increased as the ratio of CNT % increased. Porosity can be seen in Fig. 5 and 6 on the other hand, porosity was not calculated in our study.

Wear tests

Wear tests were performed on a standard disc on a machine disk with a hardness of 62 HRC, with a continuously rotating D2 set of steel plates without lubricant at room temperature. The specimen pin for the wear test is Ø10 × 10 mm and the polished wear surface for Ra roughness of 0.159 nm. The test was carried out with three trials in order to ensure its repeatability for each sample. The disk surface was grounded. Then, 0.830 μm Ra was polished to a roughness 0.830 μm Ra. sliding speed, sliding distance and load were kept constant at 1.04 m/s, 1,000 m and 10 N respectively for all tests. All the specimens were carefully cleaned with and dried. The specimens were cleaned with ethanol before and after test for measuring wear loss by a balance with an accuracy of ± 0.0001 g.

$$W_s = \frac{D_m}{qLF} * 10^9 \quad (1)$$

The wear rate was calculated using the following equation where Ws is wear rate, mm^3/Nm, D_m the mass loss of test samples during wear test of N revolutions, g, q the density of test materials, g/cm^3. L is total sliding distance, m and F the normal force on the pin, N. The total sliding distance was monitored on an auto-recorder. The worn surfaces of all the samples were examined using SEM.

The variation of wear rate with sliding distance for all samples with and without Ti64 and CNT % are shown in Fig. 7. As seen in Fig. 7, the wear rate of specimens decreases with increasing CNT % concentration in the alloy. Wear loss increased due to increased slip distance and wear rate decreased with increasing slip distance. In Fig. 7, it can be clearly seen that wear rate decreased by increased CNT % additions. Generally, with the increasing hardness dramatically decreased wear rate until CNT 4% additions. However, the lowest wear rate obtained 4% CNT addition. The most interesting result of this study was the fact that the highest wear rate was obtained in materials with the highest hardness values in the additive materials. As shown in Fig. 7, the CNT additive was increased to reduce wear loss and wear rate. The hardness observed from these observations has a significant effect on the wear behavior of the investigated materials. Wear tests show that CNT addition increases the wear resistance by 4% on average.

It is clearly displayed in Fig. 8 the effect of CNT additions on wear resistance. The highest wear resistance and hardness obtained with 4% CNT addition in Fig. 8 and 3. This observation shows that hardness has a significant effect on the wear behavior of the investigated CNT materials. The CNT 5% has a wear rate less than the CNT 4% materials.

Fig. 9 shows worn surface images of CNT additions affects s using SEM between several wear mechanisms. On the worn surface, with the exception of CNT 2% and CNT 4%, many scratches were found that were eroded by wear and plastic deformation on the surface, as shown in Figs. 9(c) and (d). In addition, many

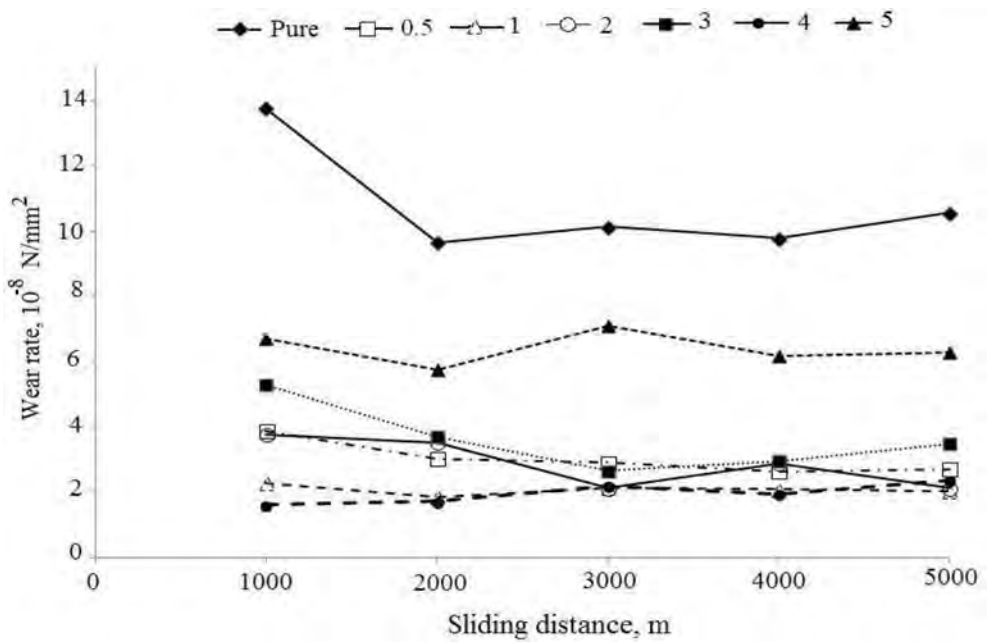

Fig. 7. Variation of wear rate with sliding distance for samples.

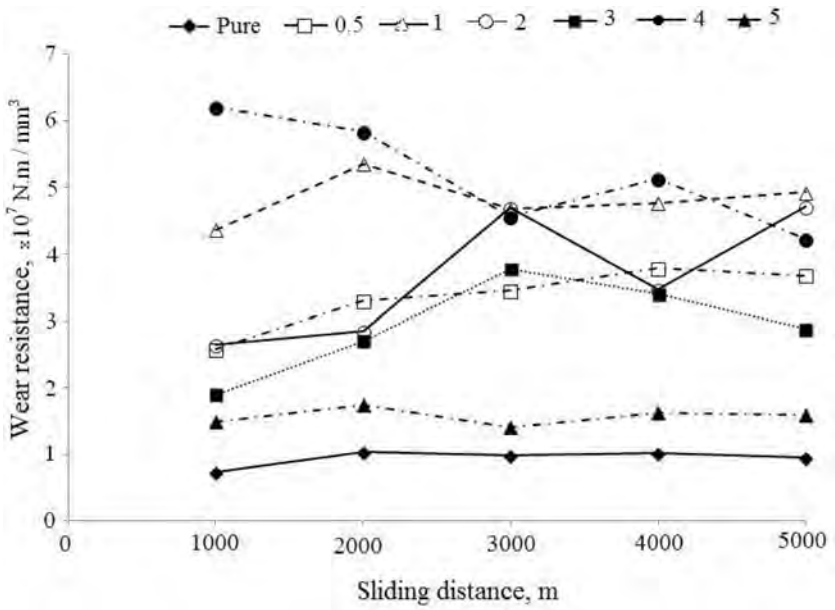

Fig. 8. Variation of wear rate with sliding distance for samples.

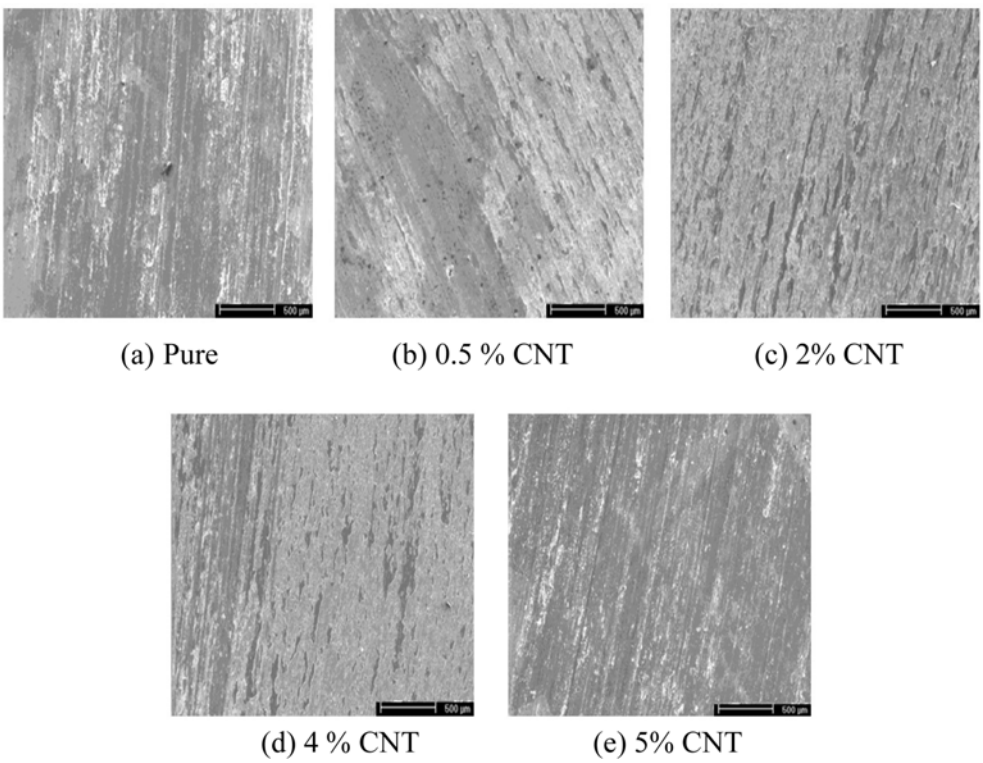

Fig. 9. Worn surfaces of titanium matrix composites.

cracks were observed on the worn surface. The growth of these cracks leads to an increase in the length of wear residues. Based on these CNT results, we can state that the amount of wear increased significantly. Otherwise, as shown in Figs. 9(a), (b) and (e), scratches were found around the surface caused by abrasive wear. The results show that the addition in CNT prevents crack propagation to a certain point as displayed in Fig. 9. This reinforcing microstructure, effectively prevented the scratching and cracking of the matrix material during wear and led to the removal of a small amount of debris. Compared to low content reinforcement (0.5%, 1, 2 CNT), this turned out to be a very different wear condition. As shown in Figs. 9(a), (b), (e), many particles were observed on the surface. In fact, it is a transfer layer of hardened particles caused by adhesion,

abrasion, and oxidation. As expected, the addition of CNT to the reinforcing bars was effective in increasing the wear resistance and friction properties of titanium. The mechanism of wear has changed after CNT 4%. The mechanism of wear was obtained pure, 0.5, 1 and 5 CNT % adhesive wear. Increased reinforcement percentages of CNT, lead to the mechanism of wear becoming abrasive wear. Therefore, the CNT 5% with the highest hardness does not achieve the highest wear resistance. This shows that the addition of additives should be at a certain CNT percentage.

Results and Discussion

The selected examples in this study are CNT-reinforced Ti64 powder produced by powder metallurgy. The mean density worth of the composites containing different ratios of CNT are as shown in Fig. 4. As the sintering temperature decreased, the density of the samples approached the theoretical density.

The XRD of samples having various CNT contents are displayed in Fig. 2. Fig. 2 shows the peaks at 2 θ of 36.4 and 40.7 belongs to the Ti6Al4V, and 25,42, and 53 belongs to the CNT. As can be seen in Fig. 2, an increase in the intensity and region of the main peak of the CNT with increasing CNT contents leads to a change.

Vickers hardness tests were performed on six different compositions and sintering temperatures of 1300 ºC. In Fig. 3, mean hardness values of the samples are given. Increasing the weight percentage of CNT also increased the stiffness of the composite. The ratio of composite materials (CNT %), Ti64 / CNT, as increased demonstrated increased micro-hardness measurements. However, the composite demonstrated abrasive wear after 4-5% weight of CNT.

Optical microscopy and SEM test were taken from the samples. In Fig. 5 and 6 displays increasing the percentage of CNT, lead to increase porosity.

The wear rate of the samples decreased rapidly due to the increase in theoretical density. However, in this case the hardness increased in the opposite direction. From 0.5 and 4 wt% CNT addition decreased sintered density, but increased hardness. Therefore, the highest wear resistance is obtained with 4 wt% CNT addition. The result of the wear test, despite being with the hardest 4 wt% CNT, wear resistance is not the highest. After 4% CNT additional, the wear mechanism has changed as displayed in Fig. 9(d) and (e). Therefore, the wear resistance is lower and identifies 4% wt CNT as the critical value. Due to 5 wt% CNT additive material having almost as much wear rate as pure material in Fig. 7. High wear resistance has been obtained in the case of adhesive wear in Fig. 7. Many scratches were found on the worn surface, except for those containing 1%, 2% and 4% CNT. In the case of CNT, the surface is worn with wear and plastic deformation, as shown in Figs. 9(c) and (d). Also, many cracks were observed on the worn surface, especially 5 wt% CNT. The spread of these cracks increases the size of the wear residues. On the other hand, as shown in Figs. 9(a), (b) and (e), we have found scratches around the worn surface caused by abrasive wear. Supplementing in CNTs have been proposed to prevent spreading of abrasive wear at certain rates.

Conclusions

The aim of this study was to investigate the density, metallographic properties and hardness of Ti64 samples supplemented with different CNT ratios as a function of sintering temperature. The densities of the samples obtained from the results of this study approach the theoretical density with increasing sintering temperatures applicable to all different ratios of CNT contents. Besides, low CNT content resulted in a closer result density. The images obtained from the SEM analysis show that the CNT particles are homogeneously dispersed in the matrix and there is no disintegration in a particular region. However, the presence of porosity at the ends of the CNT particles is present. XRD indicates that the increased CNT content causes an increase in density or area of the main peak. By increasing the weight percentage and the sintering temperature of the CNT, the hardness of the composite also increased. The effect of the sintering temperature above 1,300 ºC is lost after 4-5 wt% of CNT. The dispersion strengthening effect can be attributed to increased hardness by addition of CNT. The addition of CNT to the base alloys leads to a reduction in weight loss and wear rate during sliding wear tests. In addition, the 4 wt% Carbon Nanotube content was found to be the best way to improve friction properties. Looking at the result of the abrasion test, the wear loss is clearly reduced as the Carbon Nanotube content increases. The highest wear resistance has been obtained in the case of adhesive wear at Carbon Nanotube 4 wt % content. It is clearly demonstrated that with the increased addition of carbon nanotubes, the wear mechanisms change. The results showed that the addition of carbon nanotube up to 4 wt% lowered wear loss and increased wear resistance.

References

1. A.G. Jackson, J. Moteff, and F.H. Froes, J. Met. 31 (1979) 145.
2. L. Bolzoni, E.M. Ruiz-Navas, and E. Gordo, Mater. Sci. Forum 765 (2013) 383-387.
3. Z.Y. Ma, R.S. Mishra, and S.C. Tjong, Acta Mater. 50 (2002) 4293-4302.
4. M. Hagiwara, Y. Kaieda, Y. Kawabe, and S. Miura, ISIJ Inter 31 (1991) 922-930.
5. L. Wang, Z.B. Lang, and H.P. Shi, T. Nonferr. Metal Soc. 17 (2007) 639-643.

6. J.Q. Jiang, T.S. Lim, Y.J. Kim, and B.K. Kim, Mater. Sci. Techno. 12 (1996) 362-365.
7. A. Kelly, J. Mater. Sci. 41 (2006) 905-917.
8. S. Rawal, JOM, 53 (2001) 14-24.
9. J.S. Shelly, R. LeClaire, and J. Nichols, JOM 53[4] (2001) 18-21.
10. P. Rohatgi, JOM, 43 (1991) 10-15.
11. S. Ranganath, J. Mater. Sci., 32 (1997) 1-16.
12. M. Yamada, Mater. Sci. Eng. A. 213 (1996) 8-15.
13. S.L. Rice, S.F. Wayne, and H. Nowotny, Wear 65 (1980) 215-226.
14. S.R. Nutt and A.W. Ruff, Wear of Mater. (1983) 426-433.
15. R.B. Waterhouse and A. Iwabuchi, Wear 106 (1985) 303-313.
16. K.G. Budinski, Wear of Mater. (1991) 289-299.
17. F.M. Kutas and M.S. Misra, ASM Handbook, 18 (1992) 778-784.
18. A.P. Mercer and I.M. Hutchings, Wear, 124 (1988) 165-176.
19. I. Topcu, H.Ö. Gülsoy, N. Kadıoğlu, and A.N. Güllüoğlu, J Alloy Compd. 482 (2009) 516-521.
20. D.E. Alman and J.A. Hawk, Wear (1999) 629-639.
21. I. Topcu, B.N. Çetiner, A.N. Güllüoğlu, and H.Ö. Gülsoy, J. Chem. Soc. Pak. 42 (2020) 70-80.
22. I. Topcu, A.N. Güllüoğlu, M.K. Bilici, and H.Ö. Gülsoy, J Fac Eng Arch. Gazi Univ. 34 (2019) 141-149.
23. I. Topcu, H.Ö. Gülsoy, and A.N. Güllüoğlu, Gazi Univ. J. Sci. 32 (2019) 286-298.
24. I. Topcu, J Teh. Glas. 14 (2020) 7-14.
25. K. Saeed and N. Khan, J. Chem. Soc. Pak 37 (2015) 284-289.
26. K. Saeed, J. Chem. Soc. Pak. 32 (2010) 559-564.
27. D.H. Lee, B. Jang, C. Kim, and K.S. Lee, J. Ceram. Process. Res. 20 (2019) 499-504.
28. S.T. Hussaın, S.M. Abbas, M.A. K. Bangash, M.U. Rehman, and N. Ahmad, J. Chem. Soc. Pak. 35 (2013) 604-610.